2014

Time-resolved photoluminescence from defects in n-type GaN

Michael A. Reshchikov
Virginia Commonwealth University, mreshchi@vcu.edu

JOURNAL OF APPLIED PHYSICS **115**, 103503 (2014)

Time-resolved photoluminescence from defects in *n*-type GaN

M. A. Reshchikov[a)]
Physics Department, Virginia Commonwealth University, Richmond, Virginia 23284, USA

(Received 13 January 2014; accepted 15 February 2014; published online 10 March 2014)

Point defects in GaN were studied with time-resolved photoluminescence (PL). The effects of temperature and excitation intensity on defect-related PL have been investigated theoretically and experimentally. A phenomenological model, based on rate equations, explains the dependence of the PL intensity on excitation intensity, as well as the PL lifetime and its temperature dependence. We demonstrate that time-resolved PL measurements can be used to find the concentrations of free electrons and acceptors contributing to PL in *n*-type semiconductors. © *2014 AIP Publishing LLC*. [http://dx.doi.org/10.1063/1.4867043]

I. INTRODUCTION

Time-resolved photoluminescence (PL) can provide valuable information about point defects in semiconductors. A nonexponential decay of PL after a pulse excitation usually indicates that the PL band is associated with a donor-acceptor pair (DAP) recombination.[1] Shallow donors commonly have the largest contribution to the DAP transitions because of their larger Bohr radius. In particular, many PL bands in undoped GaN are attributed to transitions from a shallow donor to different acceptors at low temperature.[2] With increasing temperature, electrons are emitted from the shallow donor to the conduction band, and transitions from the conduction band to different acceptor levels (eA transitions) become dominant. The eA transitions are expected to cause an exponential decay of PL after a pulse excitation, with a characteristic lifetime inversely proportional to the concentration of free electrons.[2] In fact, the PL decay may remain nonexponential for a wide range of temperatures, because the eA and DAP transitions are often unresolved, and both the eA and DAP transitions contribute to the PL. However, even in such a case, the effective lifetime of PL can be defined and analyzed.[3,4]

Previously, we studied time-resolved PL from undoped *n*-type GaN and determined parameters of the defects responsible for the main PL bands in this material.[3–6] One of the well-studied bands is the blue luminescence (BL) band with a maximum at 2.9 eV. This band is attributed to the Zn_{Ga} acceptor.[2] The BL band intensity is independent of temperature at low temperatures, and it is quenched with an activation energy of about 350 meV at temperatures higher than a characteristic temperature T_0 ($T_0 \approx 200$ K for the BL band). In the Arrhenius plot, T_0 is defined as the temperature where two lines, corresponding to the temperature-independent and exponential parts, cross when extrapolated.[7,8] The PL lifetime for the BL band decreases with increasing concentration of free electrons, and it varies slowly with temperature for $T < T_0$. At $T > T_0$, the measured PL lifetime decreases with some activation energy in the Arrhenius plot.[4,6] No quantitative description of the temperature dependence of the PL lifetime was given in these works.

The temperature dependence of the PL lifetime for defects in GaN and other semiconductors has been studied in very few works. Kwon *et al.*[9] observed that the lifetime of the yellow luminescence (YL) band in GaN decreases with Si doping but is nearly independent of temperature between 10 and 300 K. Gil *et al.*[10] reported on a small increase of the PL lifetime with increasing temperature from 8 to 300 K for the blue band peaking at 2.6 eV in GaN doped with As. As for the defect-related PL in other semiconductors, in some cases, the PL lifetime has the same or similar temperature dependence as the PL intensity,[11] whereas in other examples these dependencies differ substantially.[12,13] Recently, we demonstrated that the value of T_0 in high-resistivity GaN strongly depends on the absolute internal quantum efficiency (IQE) of PL.[7] It is unclear *a priori* if the temperature dependencies of PL intensity and PL lifetime are identical to each other or not, and how the PL lifetime depends on the absolute IQE of PL.

In this work, we present the experimental data on time-resolved PL in *n*-type GaN samples and provide a model that explains the temperature dependence of the PL lifetime associated with defects.

II. EXPERIMENT

Basic information about the samples analyzed in this work is given in Table I. Two undoped GaN samples and one Si-doped sample (1011, 1611, and 2015, respectively) were grown by hydride vapor phase epitaxy (HVPE) at TDI, Inc. Three GaN layers co-doped with Si and Zn (samples 1140, 1142, and 1154) were grown by the metalorganic vapor phase epitaxy (MOVPE) method at TUBS (Germany). Undoped GaN layers (samples 6615 and 6623) were grown by molecular beam epitaxy (MBE) at VCU. All the GaN layers were grown on *c*-plane sapphire substrates.

Steady-state PL was excited with a 50 mW He-Cd laser, dispersed by a 1200 rules/mm grating in a 0.3-m monochromator, and was detected by a cooled photomultiplier tube. Time-resolved PL was excited with a pulsed nitrogen laser (1 ns pulses with repetition frequency of 6 Hz, and 337 nm wavelength) and analyzed with an oscilloscope. A closed-cycle optical cryostat was employed to achieve sample temperatures between 15 and 320 K. The PL spectra were

[a)]Electronic mail: mreshchi@vcu.edu

TABLE I. Parameters of GaN samples.

Sample	Growth method	Producer	Doping	Active layer thickness (μm)	n from the Hall effect (cm^{-3})	n from PL[a] (cm^{-3})
1011	HVPE	TDI	…	6	1.5×10^{17}	1.3×10^{17}
1611	HVPE	TDI	…	300	2×10^{16}	5×10^{16}
2015	HVPE	TDI	Si	5	3×10^{17}	4.4×10^{17}
1154	MOVPE	TUBS	Si, Zn	0.2	6×10^{18}	1.8×10^{19}
1142	MOVPE	TUBS	Si, Zn	0.2	1.0×10^{19}	1.2×10^{19}
1140	MOVPE	TUBS	Si, Zn	0.2	7.5×10^{18}	4.5×10^{18}
6615	MBE	VCU	…	2	N/A	1×10^{17}
6623	MBE	VCU	…	2	3×10^{18}	3×10^{18}

[a]Calculated by using Eq. (3) with $C_{n1} = 1.5 \times 10^{-13}$ cm^3/s and $C_{n1} = 8 \times 10^{-13}$ cm^3/s for the BL band and UVL band, respectively.

corrected for the response of the optical system by comparing the spectrum of a tungsten lamp with a standard spectrum. To find the absolute IQE for a particular PL band in the steady-state PL experiments, we compared the integrated intensity of this band with the PL intensity obtained from a standard GaN sample previously calibrated[8] and measured under identical conditions and with a known excitation power density P_{exc}. The intensity of the incident laser light at the sample surface, denoted as P_0, was determined from P_{exc} by converting Watts into the number of photons.

III. RESULTS

A. Steady-state PL spectra

The PL spectra from the studied samples at 100 K are shown in Fig. 1. In two HVPE-grown GaN samples, the BL band was one of the dominant defect-related bands [Fig. 1(a)]. The BL band is attributed to transitions from the conduction band (or from shallow donors at low temperatures) to the Zn_{Ga} acceptor, which has an energy level at about 0.35 eV above the valence band maximum.[2,14,15] It is established that a Zn contamination at a level of only $10^{15} - 10^{16}$ cm^{-3} results in a very intense BL band, with an IQE up to 30%.[7] In addition to the BL band and the exciton emission lines located close to the GaN bandedge, the PL spectra from the HVPE-grown GaN contained an ultraviolet luminescence (UVL) band with the main peak at ~3.28 eV, followed by LO phonon replicas, and a broad red luminescence (RL) band with a maximum at 1.8 eV [Fig. 1(a)]. The identity of the defects responsible for the UVL and RL bands in undoped GaN is not established.

The BL band is also the dominant band in the PL spectrum of the GaN:Si,Zn samples grown by MOVPE [Fig. 1(b)]. No UVL band could be detected in these samples. Finally, the spectra from the MBE-grown GaN samples analyzed in this work contain a very intense UVL band, with an IQE reaching 80% for sample 6623.[8] The identity of the shallow acceptor responsible for the UVL band in these samples is also not established.

Figure 2 shows an example of the evolution of the PL spectrum with increasing temperature for an undoped GaN sample. We observe a transformation of the UVL band, which is typical for n-type GaN: the shallow DAP band with a main peak at 3.262 eV gives way to the eA band with a main peak at 3.285 eV at about 50 K (Fig. 2). This transformation is explained by the thermal emission of electrons from shallow donors to the conduction band and their recombination with holes bound to the Zn_{Ga} acceptors. Note that the integrated intensity of the UVL band remains almost unchanged up to $T \approx 100$ K. The UVL band is quenched at higher temperatures and completely disappears at 200 K (Fig. 2). The BL band intensity is independent of temperature up to $T \approx 200$ K, and is quenched at higher temperatures (not shown).

B. Decay of photoluminescence

The evolution of the BL intensity after a pulse excitation for three GaN samples at 180 K is shown in Fig. 3(a). The

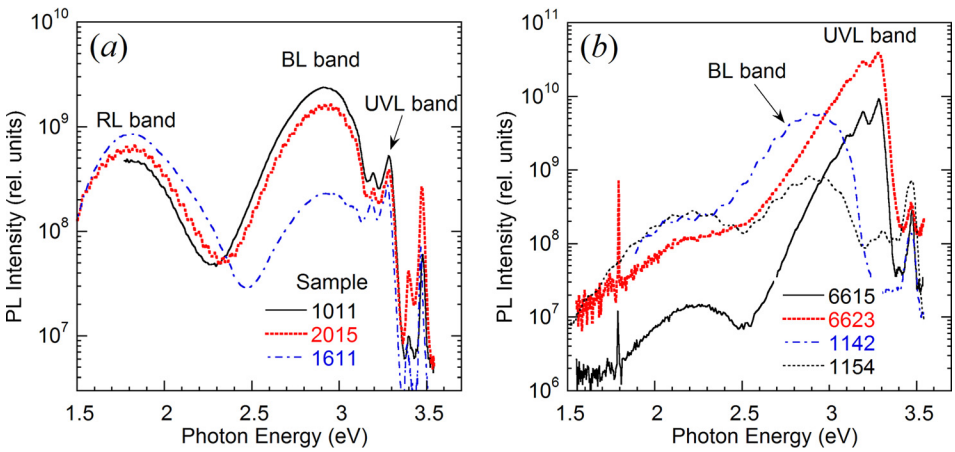

FIG. 1. PL spectra from GaN samples at $T = 100$ K and $P_{exc} = 3 \times 10^{-4}$ W/cm^2. (a) HVPE-grown samples and (b) MBE- and MOVPE-grown samples.

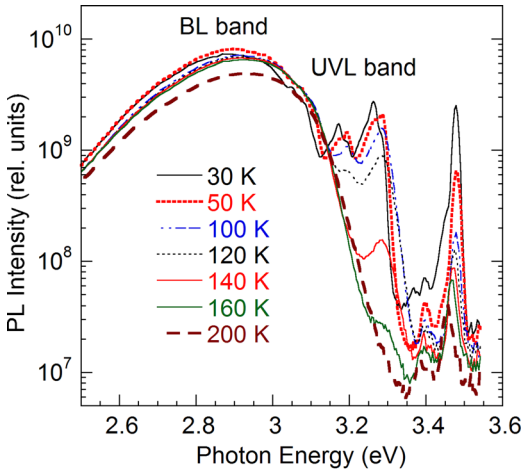

FIG. 2. Evolution of PL spectrum with increasing temperature for undoped GaN (sample 1011). $P_{exc} = 3 \times 10^{-5}$ W/cm^2.

PL decay is nearly exponential at this temperature. Figure 3(b) shows the product of the PL intensity and elapsed time plotted as a function of time delay. Following an approach suggested in Ref. 4, the characteristic lifetime of PL, τ, is defined as the position of the maximum in this dependence [shown with arrows in Fig. 3(b)]. From PL decays at different photon energies, we reconstructed the PL spectra at selected time delays and compared them to the steady-state PL spectra (Fig. 4). This comparison is needed to prove that the PL decay analyzed in the time-resolved PL experiment is related to a particular PL band and not to other PL bands contributing at the same photon energy. For example, we see that the time-resolved PL data between 1.8 and 2.4 eV in Fig. 4(a) are unrelated to the RL and BL bands, and it reveals the YL band with a maximum at 2.2 eV, which is not resolved in our steady-state PL experiments.

Figure 5 shows the dependence of the PL intensity on the excitation intensity for the BL band in time-resolved PL measurements. At low excitation intensities, the PL intensity increases linearly with P_0, and at high excitation intensity, a complete or partial saturation is observed [Fig. 5(a)]. The saturation of the PL signal is attributed to the saturation of defects with photogenerated holes. The characteristic excitation intensity at which the saturation begins does not depend on temperature [Fig. 5(b)]. The decay of PL in our experiments was measured at relatively low excitation intensities, when the defects participating in the PL process are not saturated with holes. However, the characteristic lifetime remained nearly the same for the entire range of used excitation intensities.

C. Temperature dependence of PL lifetime

The temperature dependencies of the PL lifetime for selected samples are shown in Fig. 6. As the temperature increases from 100 to 180 K, the PL lifetime of the BL band decreases slowly for the samples with a low concentration of free electrons (samples 1611, 1011, and 2015), and it is independent of temperature for the degenerate GaN (sample 1142). At higher temperatures, the PL lifetime decreases with a slope revealing an activation energy E_A in the Arrhenius plot (Fig. 6). It is interesting to note that, while the PL decayed faster at higher temperatures, the initial PL intensity (immediately after a laser pulse) remained unchanged (Fig. 7).

In Fig. 8, the PL lifetimes for the BL band in three samples (filled symbols) are normalized to their values at low temperatures (120–140 K) and compared with the normalized PL intensities (empty symbols). For a given sample, the values of T_0 determined from the temperature dependencies of the PL lifetime and PL intensity are almost identical. However, T_0 is quite different for different samples (Table II). At $T > T_0$, both the PL lifetime and PL intensity decrease with an activation energy of about 300–350 meV for the BL band in all the samples.

Figure 9 compares the normalized temperature dependencies of the PL lifetime and PL intensity for the UVL band in two samples. Again, we see very similar temperature behavior of the PL lifetime and PL intensity for a given sample and different values of T_0 for different samples. The activation energy of the dependencies in the region of thermal quenching ($T > T_0$) is about 150 meV for the UVL band. To explain the temperature and excitation-intensity behavior of the defect-related PL described above, we developed a phenomenological model for the defect-related time-resolved PL.

IV. THEORY

A. Rate equations model

Let us consider an n-type semiconductor which contains shallow donors D with the concentration N_D and ionization

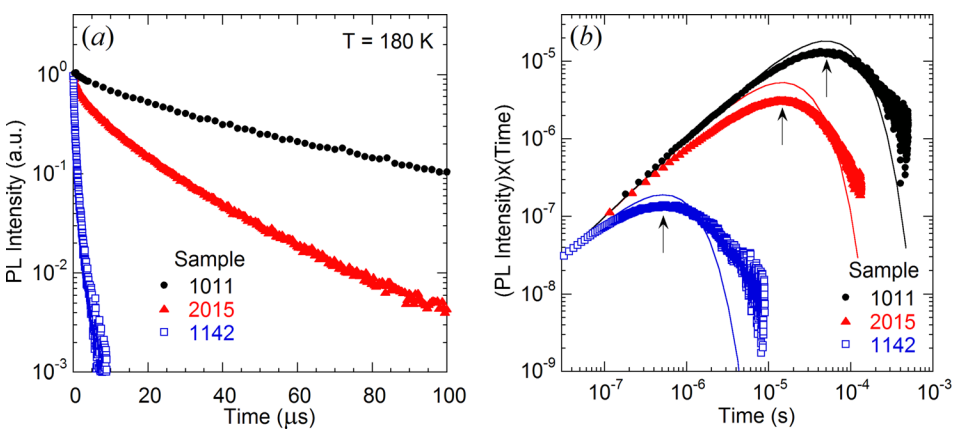

FIG. 3. Decay of PL after a laser pulse at 180 K for the BL band (at 2.9 eV) in GaN. (a) PL intensity as a function of elapsed time. (b) Product of PL intensity and time as a function of time. Arrows show characteristic lifetimes τ determined from the position of maxima in the $I^{PL}t$ dependencies. Solid curves are dependencies of the form $e^{-t/\tau}t$ with $\tau = 5.5 \times 10^{-7}$, 1.5×10^{-5}, and 5×10^{-5} s for samples 1142, 2015, and 1011, respectively.

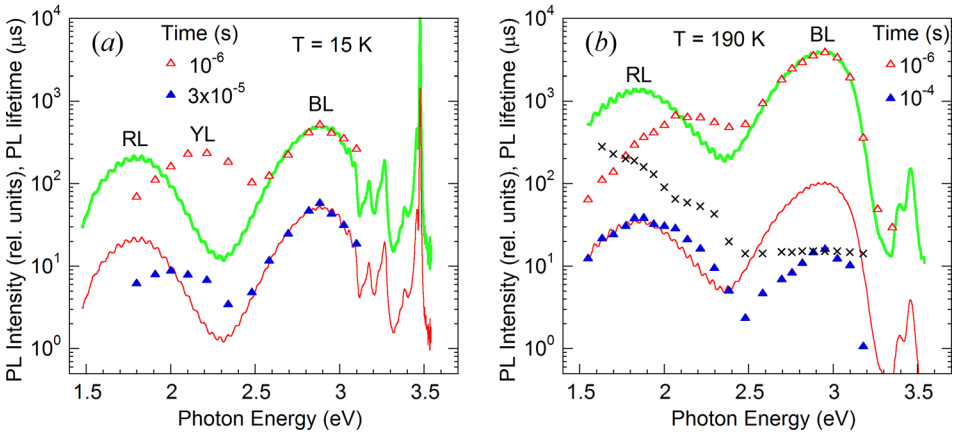

FIG. 4. PL spectra for Si-doped GaN (sample 2015). (a) $T = 15$ K, (b) $T = 190$ K. Empty and filled triangles show PL spectrum obtained from time-resolved PL at the indicated time delays. Crosses show spectral dependence of τ at 190 K. Solid curves show steady-state PL spectra at $P_{exc} = 3 \times 10^{-5}$ W/cm^2, shifted vertically arbitrarily for comparison with the time-resolved PL spectra.

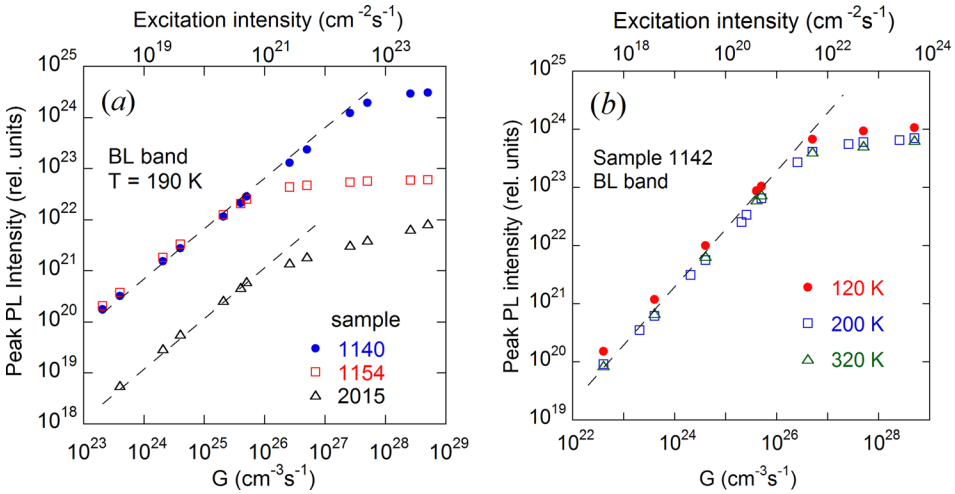

FIG. 5. Dependence of PL intensity after the laser pulse on excitation intensity for the BL band in GaN samples. (a) Three samples at $T = 190$ K. (b) Sample 1142 at different temperatures. Dashed lines show linear dependencies.

energy E_D, a selected acceptor A with concentration N_1 and ionization energy E_1, and several other types of defects with concentrations N_i $(i = 2, ..., k)$ that participate in electron-hole recombination. These defects include radiative defects and centers of nonradiative recombination. Under illumination, electron-hole pairs are produced with a generation rate G per unit volume. For simplicity, we will assume in this section that G is constant within an active layer of thickness α^{-1}, where α is the absorption coefficient, and $G = 0$ beyond this layer. The concentrations of free electrons and holes are n and p, respectively. We use the traditional description of transition rates as the product of the concentrations of available carriers and available empty sites, multiplied by a constant factor called the capture coefficient.[16,17] In particular, the rate term $C_{p1}N_1^- p$ describes the capture of free holes by the negatively charged acceptor A, with C_{p1} being the hole-capture coefficient for the acceptor. Similarly, $C_{n1}N_1^0 n$, where C_{n1} is the electron-capture coefficient, describes the

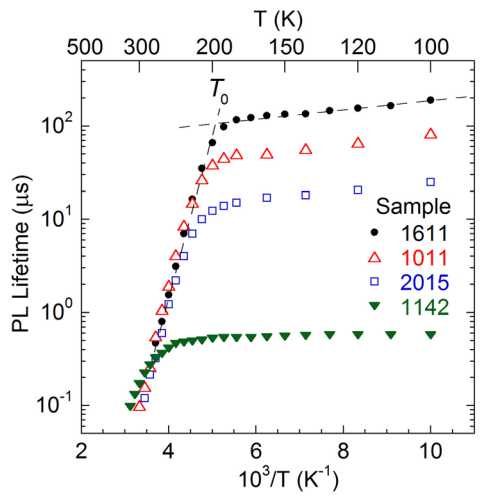

FIG. 6. Temperature dependence of PL lifetime for the BL band in GaN. An example of determination of T_0 for sample 1611 is shown with dashed lines.

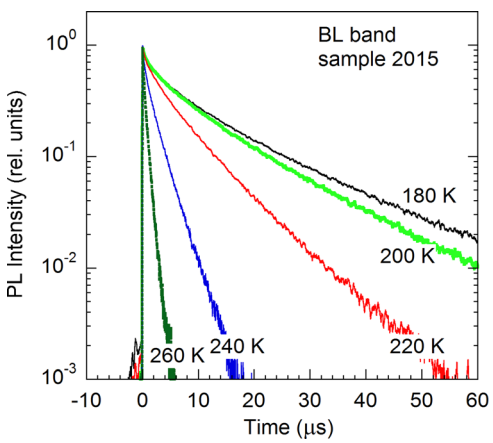

FIG. 7. Decay of BL band intensity after a pulse excitation at different temperatures. Sample 2015.

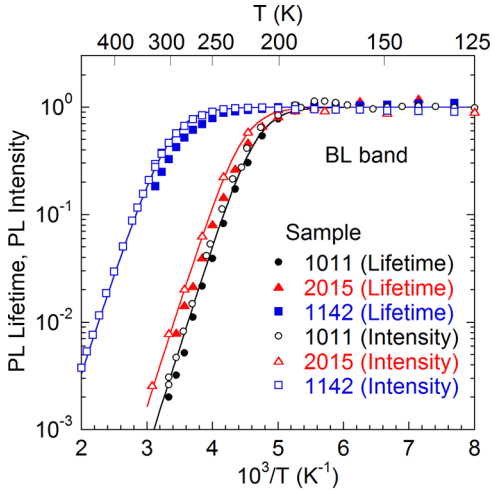

FIG. 8. Temperature dependence of PL intensity and PL lifetime for the BL band in undoped GaN (sample 1011), GaN:Si (sample 2015), and GaN:Si,Zn (sample 1142), normalized at 125 K. Solid lines are calculated using Eq. (39) with $C_{p1} = 7 \times 10^{-7}$ cm^3/s, $N_v = 3.2 \times 10^{15} T^{3/2}$ cm^{-3}, and other parameters given in Table II.

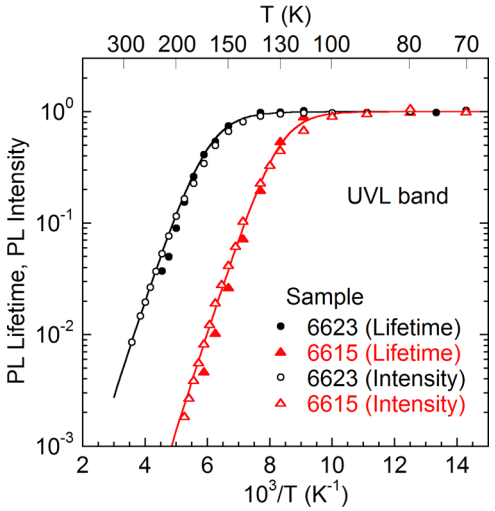

FIG. 9. Temperature dependence of PL intensity and PL lifetime for the UVL band in MBE-grown GaN. Solid lines are calculated using Eq. (39) with the following parameters: $\eta_{10} = 0.85$, $\tau_{10} = 0.4$ μs, $E_1 = 130$ meV (sample 6623); $\eta_{10} = 0.15$, $\tau_{10} = 16.5$ μs, $E_1 = 150$ meV (6615). $C_{p1} = 7 \times 10^{-8}$ cm^3/s for both samples.

recombination between free electrons and holes bound to the acceptor A. We will neglect the DAP recombination, what is typically justified for temperatures above 100 K in n-type GaN. Then, the PL intensity via the acceptor with $i = 1$, I_1^{PL}, and its absolute IQE, η_1, can be expressed as

$$I_1^{PL} = C_{n1} N_1^0 n = \frac{N_1^0}{\tau_{10}} \tag{1}$$

and

$$\eta_1 = \frac{I_1^{PL}}{G} = \frac{N_1^0}{\tau_{10} G}, \tag{2}$$

respectively. Here, the parameter τ_{10}, introduced as

$$\tau_{10} = (C_{n1} n)^{-1}, \tag{3}$$

has the meaning of the PL lifetime in the low-temperature limit as will be shown later.

TABLE II. Parameters for the BL band in GaN samples.

Sample	1011	1611	2015	1154	1142	1140
E_1 (meV)	345	348	340	345	310	290
T_0 (K)	215	205	225	290	295	305
T_2 (K)	745	710	650	590	705	1090
η_{10}	0.2	0.07	0.2	0.4	0.94	0.96
N_1 from SS-PL (10^{17} cm^{-3})	0.2	0.07	0.1	0.05	3	30
N_1[a] from TR-PL (10^{17} cm^{-3})	0.3	N/A	0.12	0.1	1.7	25
$1/Q_1$ at $T = 190$ K (μs)	480	580	360	480	40	17
τ_{10} (μs)	50	130	15	0.36	0.55	1.48
τ_{20}[b] (ps)	10	14	24	57	8	0.5

[a]From the fit of the experimental data with Eq. (37).
[b]Calculated by using Eq. (8) with $C_{p1} = 7 \times 10^{-7}$ cm^3/s and the value of N_1 determined from the time-resolved (TR-PL) data except for sample 1611, for which N_1 was determined from the steady-state PL (SS-PL).

The rate of change of the concentration of holes bound to the acceptor with $i = 1$ is given by

$$\frac{dN_1^0}{dt} = C_{p1} N_1^- p - C_{n1} N_1^0 n - Q_1 N_1^0. \tag{4}$$

The first term on the right side of this equation describes the capture of free holes by the negatively charged acceptors. Note that N_1^- can be replaced with N_1 for low excitation intensities (when the acceptors are not saturated with photogenerated holes) in an n-type semiconductor.[7] The second term on the right side describes the recombination of free electrons with bound holes, which is the observed PL. The last term in Eq. (4) describes the thermal emission of holes from the acceptor to the valence band with the rate Q_1,[7,8]

$$Q_1 = C_{p1} N_v g^{-1} \exp\left(-\frac{E_1}{kT}\right), \tag{5}$$

where N_v is the effective density of states in the valence band, g is the degeneracy factor of the acceptor level (assumed to be equal to 2 for acceptors in GaN), T is the temperature, and k is Boltzmann's constant.

The rate of change of the hole concentration in the valence band is given by

$$\frac{dp}{dt} = G - \sum_{i=1}^{k} C_{pi} N_i p + Q_1 N_1^0. \tag{6}$$

Here, the term $C_{pi} N_i p$ in the sum describes the capture of free holes by the ith type of defects with concentration N_i. For generality, we can include the near-bandedge emission in this sum as one of the recombination channels by formally assigning $C_{pi} = B$ and $N_i = n$, where the rate coefficient B includes both the exciton and free electron-hole recombination components.[18]

The absolute IQE of PL, $\eta_1 = I_1^{PL}/G$, caused by the recombination of carriers via the acceptor A, in the limit of low temperatures (when $Q_1 \approx 0$), can be expressed as[7,8]

$$\eta_1(T \to 0) \equiv \eta_{10} = \frac{C_{p1}N_1}{\sum_{i=1}^{k} C_{pi}N_i}. \quad (7)$$

It is also useful to define the characteristic lifetime of holes in the valence band in the limit of low temperatures, τ_{20}, as

$$\tau_{20} = \frac{1}{\sum_{i=1}^{k} C_{pi}N_i} = \frac{\eta_{10}}{C_{p1}N_1}. \quad (8)$$

Accounting for Eqs. (3) and (8), Equation (4) can be re-written as

$$\frac{dN_1^0}{dt} = -\left(\frac{1}{\tau_{10}} + Q_1\right)N_1^0 + \frac{\eta_{10}}{\tau_{20}}\left(1 - \frac{N_1^0}{N_1}\right)p. \quad (9)$$

On the other hand, the change in the concentrations of free holes during the excitation ($G > 0$) and after an excitation pulse ($G = 0$) can be expressed from Eq. (6), accounting for Eq. (8), as

$$\frac{dp}{dt} = G + Q_1N_1^0 - \frac{p}{\tau_{20}} \quad (10)$$

and

$$\frac{dp}{dt} = Q_1N_1^0 - \frac{p}{\tau_{20}}, \quad (11)$$

respectively. Below, we will analyze the carrier dynamics for the cases of $G > 0$ (during illumination) and $G = 0$ (after the illumination).

B. Increase in the concentration of free and bound holes during illumination

It follows from analysis of Eqs. (9) and (10) that the term $Q_1N_1^0$ in Eq. (10) can be neglected for the ranges of temperature and excitation intensity used in our experiments and for the typical lifetimes of free holes in GaN (smaller than 10^{-9} s). Then, the solution of Eq. (10) is

$$p = G\tau_{20}[1 - \exp(-t/\tau_{20})]. \quad (12)$$

According to Eq. (12), the concentration of free holes increases linearly with time, as $p = Gt$, and it saturates at $p = G\tau_{20}$ when $t \to \infty$. For the studied GaN samples, the time at which the saturation begins ($t \approx \tau_{20}$) is much smaller than the length of our laser pulse (1 ns).

To obtain simple analytical expressions describing the time evolution of the concentration of holes bound to the acceptor, $N_1^0(t)$, we can present Eq. (12) as consisting of two parts: a linear dependence, $p = Gt$ at $t \le \tau_{20}$, and the saturation region, $p = G\tau_{20}$ at $t \ge \tau_{20}$. At $t \le \tau_{20}$, the concentration of holes bound to the acceptor remains low, and the term N_1^0/N_1 in Eq. (9) can be neglected. Then, by substituting $p = Gt$ into Eq. (9), we find the following solution for $N_1^0(t)$ at $t \le \tau_{20}$

$$N_1^0 = \frac{\eta_{10}G}{2\tau_{20}}t^2, \quad (13)$$

which gives $N_1^0 = 0.5\eta_{10}G\tau_{20}$ at $t = \tau_{20}$. For $t \ge \tau_{20}$, we will replace p with $G\tau_{20}$ in Eq. (9). Then, the solution for $N_1^0(t)$ at $t \ge \tau_{20}$ can be found as

$$N_1^0 = \frac{\eta_{10}G}{\lambda}\left\{1 - \left(1 - \frac{\lambda\tau_{20}}{2}\right)\exp[-\lambda(t - \tau_{20})]\right\}, \quad (14)$$

where

$$\lambda = \frac{1}{\tau_{10}} + Q_1 + \frac{\eta_{10}G}{N_1}. \quad (15)$$

Figure 10 shows the $p(t)$ and $N_1^0(t)$ dependencies for low and high excitation intensities calculated with Eqs. (12)–(14). We can see that at $t > \tau_{20}$, the concentration of holes bound to the acceptor increases linearly with time and saturates at $N_1^0(t) \approx N_1$ when $t \gg \lambda^{-1}$.

Next, we find the concentrations of free and bound holes at the end of a laser pulse, at $t = t_L$, where t_L is the length of the laser pulse. These values will be the initial points for the evolution of the free and bound hole concentrations after the pulse and will be labeled as $p(0)$ and $N_1(0)$, respectively. If $t_L > \tau_{20}$ (which is always satisfied in our experiments on GaN), the concentration of free and bound holes at the end of the pulse are

$$p(0) = G\tau_{20} \quad (16)$$

and

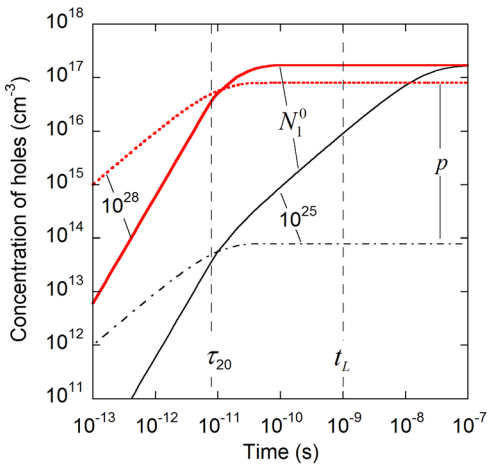

FIG. 10. Evolution of the concentration of free holes (p) and bound holes (N_1^0) after the excitation light is turned on at $t = 0$, for low ($G = 10^{25}$ cm^{-3}s^{-1}) and high ($G = 10^{28}$ cm^{-3}s^{-1}) excitation intensities. Dash-dotted and dotted lines show p calculated with Eq. (12). Solid lines show N_1^0 calculated with Eq. (13) at $t \le \tau_{20}$ and with Eq. (14) at $t \ge \tau_{20}$. Parameters are taken for sample 1142 (Table II) and for $T = 190$ K. Vertical dashed lines show the characteristic lifetime τ_{20} and duration of the laser pulse t_L in our time-resolved PL experiments.

$$N_1^0(0) = \frac{\eta_{10} G}{\lambda}\left\{1 - \left(1 - \frac{\lambda\tau_{20}}{2}\right)\exp[-\lambda(t_L - \tau_{20})]\right\}, \quad (17)$$

respectively. The dependence of $N_1^0(0)$ on the electron-hole generation rate (or laser intensity) is shown in Fig. 11. It consists of a linear dependence at low G, which for $\lambda(t_L - \tau_{20}) \ll 1$ can be approximated by

$$N_1^0(0) = \eta_{10} G\left(t_L - \frac{\tau_{20}}{2}\right), \quad (18)$$

and it saturates at $N_1^0(0) \approx N_1$ for $\lambda(t_L - \tau_{20}) \gg 1$. The characteristic generation rate G_0 can be defined as G at which the linear dependence given with Eq. (18), when extrapolated, crosses the value of N_1, i.e.,

$$G_0 = \frac{N_1}{\eta_{10}\left(t_L - \frac{\tau_{20}}{2}\right)} \approx \frac{N_1}{\eta_{10} t_L}. \quad (19)$$

Note that in the steady-state PL, the saturation of PL begins at[2]

$$G_0 \approx \frac{N_1}{\eta_{10}\tau_{10}}. \quad (20)$$

From Eq. (1), accounting for Eq. (17), the PL intensity in the end of a laser pulse is

$$I_1^{PL}(0) = \frac{N_1^0(0)}{\tau_{10}} = \frac{\eta_{10} G}{\lambda\tau_{10}}\left\{1 - \left(1 - \frac{\lambda\tau_{20}}{2}\right)\exp[-\lambda(t_L - \tau_{20})]\right\}. \quad (21)$$

Since the PL decays after the pulse, $I_1^{PL}(0)$ will be called "the peak intensity," hereafter. For typical parameters of the defects in GaN and the conditions used in our experiments, $\lambda(t_L - \tau_{20}) \ll 1$. In this case, no temperature dependence of the $I_1^{PL}(0)$ could be noticed; i.e., for a given excitation intensity, the peak PL intensity is practically independent of temperature, in agreement with the experimental data shown in Fig. 7.

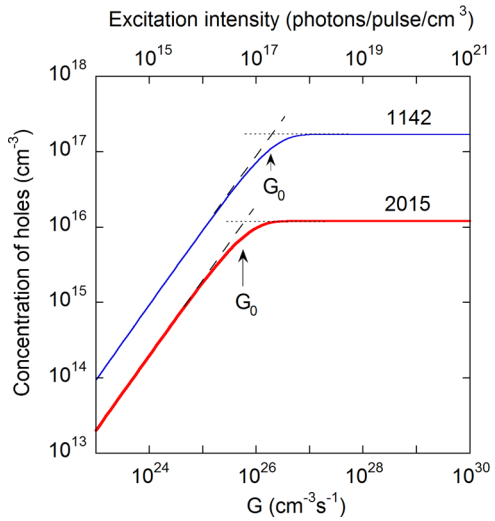

FIG. 11. Dependence of the concentration of bound holes, N_1^0 (0), on excitation intensity at the end of the laser pulse. Solid curves are calculated with Eq. (17), dashed curves are calculated with Eq. (18), and horizontal dotted lines indicate N_1. Parameters are used from Table II for samples 1142 and 2015. Arrows show the characteristic generation rate at which the saturation of the acceptors with holes begins.

C. PL decay after a pulse excitation

When the excitation intensity is low enough, so that $G \ll G_0$ [or $N_1^0(0) \ll N_1$], we can neglect the N_1^0/N_1 term in Eq. (9), which results in

$$\frac{dN_1^0}{dt} = -\left(\frac{1}{\tau_{10}} + Q_1\right)N_1^0 + \frac{\eta_{10}}{\tau_{20}}p. \quad (22)$$

Among the possible solutions of a linear system of Eqs. (11) and (22) are

$$N_1^0(t) = N_1^0(0)\exp(-t/\tau) \quad (23)$$

and

$$p(t) = p(0)\exp(-t/\tau), \quad (24)$$

where $N_1^0(0)$ and $p(0)$, given with Eqs. (16) and (17), are the concentrations of bound and free holes before ceasing the excitation light at $t = 0$. By substituting Eqs. (23) and (24) into Eqs. (11) and (22), we obtain a quadratic equation for τ

$$\tau^2[1 + (1 - \eta_{10})Q_1\tau_{10}] - \tau[\tau_{20}(1 + Q_1\tau_{10}) + \tau_{10}] + \tau_{10}\tau_{20} = 0. \quad (25)$$

Both roots of this equation, τ_1 and τ_2, have a physical meaning and will be used below. Figure 12 shows the temperature dependence of τ_1 and τ_2. At very low temperatures, when $T < T_0$ or $\tau_{20} \ll \tau_{10} \ll {Q_1}^{-1}$, then $\tau_1 = \tau_{10}$ and $\tau_2 = \tau_{20}$. Above a critical temperature T_0, τ_1 decreases exponentially with increasing temperature, while τ_2 remains constant. Above a very high temperature T_2, which can be found from the condition $\tau_{20} = {Q_1}^{-1}$, τ_1 is constant and τ_2 decreases

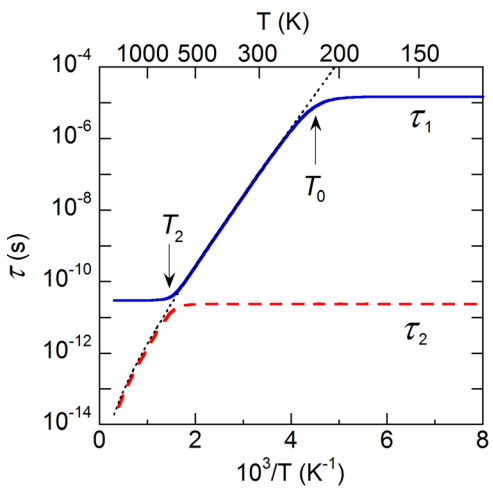

FIG. 12. Lifetimes τ_1 and τ_2 found as the roots of Eq. (25). Dotted line is the dependence $\tau = (1 - \eta_{10})^{-1}{Q_1}^{-1}$. The parameters correspond to sample 2015 and are given in Table II. $N_v = 3.2 \times 10^{15} T^{3/2}$ cm^{-3}, $g = 2$, and $C_{p1} = 7 \times 10^{-7}$ cm^3/s.

exponentially. For a wide range of temperatures ($T \ll T_2$), where $\tau_{20} \ll \tau_{10}, {Q_1}^{-1}$, the approximate solutions of Eq. (25) are

$$\tau_1 = \frac{\tau_{10}}{1 + (1 - \eta_{10})\tau_{10}Q_1} \tag{26}$$

and

$$\tau_2 = \tau_{20}. \tag{27}$$

For $T \gg T_0$, where $\tau_{20}, {Q_1}^{-1} \ll \tau_{10}$, the approximate solutions of Eq. (25) are

$$\tau_1 = \frac{\tau_{20}}{(1 - \eta_{10})}\left(1 + \frac{1}{\tau_{20}Q_1} - \frac{1 - \eta_{10}}{1 - \tau_{20}Q_1}\right) \tag{28}$$

and

$$\tau_2 = \frac{\tau_{20}}{1 + \tau_{20}Q_1}. \tag{29}$$

In our experiments, the temperature has never achieved T_2 (Table II); therefore, we will use only Eqs. (26) and (27) below. Since both roots of Eq. (25) satisfy Eqs. (11) and (22), the solutions of these equations can be found as

$$N_1^0(t) = A_1 \exp(-t/\tau_1) + A_2(-t/\tau_2) \tag{30}$$

and

$$p(t) = B_1 \exp(-t/\tau_1) + B_2 \exp(-t/\tau_2). \tag{31}$$

By substituting Eqs. (30) and (31) into Eqs. (11) and (22), accounting for Eqs. (16), (18), (26), and (27), we can find coefficients A_1, A_2, B_1, and B_2 for the case of $T \ll T_2$ (or $\tau_{20} \ll \tau_{10}, {Q_1}^{-1}$) and derive the following expressions for decays of PL intensity and the concentration of free holes after a laser pulse:

$$I_1^{PL}(t) = \frac{N_1^0(t)}{\tau_{10}} = \frac{\eta_{10}Gt_L}{\tau_{10}}\left[\exp(-t/\tau_1) - \frac{\tau_{20}}{t_L}\exp(-t/\tau_{20})\right] \tag{32}$$

and

$$p(t) = G\tau_{20}\left[\delta \exp(-t/\tau_1) + (1 - \delta)\exp(-t/\tau_{20})\right], \tag{33}$$

where

$$\delta = Q_1\tau_{20}\left(1 + \eta_{10}\frac{t_L}{\tau_{20}} - \eta_{10}\right), \tag{34}$$

and τ_1 is given with Eq. (26).

When a laser pulse is long enough ($t_L \gg \tau_{20}$), PL intensity decays exponentially after a laser pulse, with the characteristic time constant τ_1

$$I_1^{PL}(t) \approx \frac{\eta_{10}Gt_L}{\tau_{10}}\exp(-t/\tau_1). \tag{35}$$

At $T < T_0$, the PL lifetime is independent of temperature and is equal to τ_{10}. The thermal quenching of PL begins at $T > T_0$, where T_0 can be found from the condition $(1 - \eta_{10})\tau_{10}Q_1 = 1$.[7,8] The PL lifetime also decreases exponentially with increasing temperature at $T > T_0$, so that the activation energy of this decrease in the Arrhenius plot is E_1. The concentration of free holes at $T < T_0$ decreases very quickly, with the characteristic time constant τ_{20}. However, at $T \gg T_0$, the slow component (with time constant τ_1) may appear in the decay of the free-hole concentration, when the parameter δ in Eq. (33) is no longer negligible.

Figure 13 shows the calculated decays of the PL intensity and time dependencies of the free-hole concentration for selected temperatures. The parameters for the calculations are chosen to describe PL transients of the BL band in two characteristic GaN samples: a moderately doped sample 2015 and a degenerate GaN sample 1142, for which $T_0 = 225$ and 295 K, respectively. The PL intensity at low temperatures ($T < T_0$) decays exponentially after a laser pulse with the characteristic time constant τ_{10} defined with Eq. (3) [the curves for $T = 100$ and 200 K coincide in Figs. 13(a) and 13(b)]. At $T > T_0$, the PL decay is still exponential but the characteristic PL lifetime τ_1, given by Eq. (26), decreases with increasing temperature as $\tau_1 \propto \exp(E_1/kT)$ [Figs. 13(a) and 13(b)]. The concentration of holes in the valence band at low temperatures decreases much faster than the PL intensity, with the characteristic time constant τ_{20} [the $T = 100$ K curve in Figs. 13(c) and 13(d)]. At higher temperatures, the time dependence of the concentration of free holes has two exponential regions: a fast component with the time constant τ_{20} and a slow component with the time constant τ_1 [Figs. 13(c) and 13(d)]. The contribution of the latter increases with increasing temperature.

V. DISCUSSION

A. Dependence of PL intensity on excitation intensity

We have estimated for our setup that the maximal intensity of the incident light from the nitrogen laser during the 1 ns pulse is $P_0 = 5 \times 10^{23}$ photons per cm^2 per s at the sample surface. In an approximation hereafter referred to as a "simple model," we assume that the laser light is absorbed in the near-surface layer with effective thickness of $d = \alpha^{-1}$, where $\alpha \approx 10^5$ cm^{-1} for GaN at 337 nm [Ref. 19]. Assuming that the generation rate G is constant in this layer (i.e., $G = \alpha P_0$), we estimate that our nitrogen laser, without attenuation, generates $G = 5 \times 10^{28}$ electron-hole pairs in a cubic centimeter per second during the pulse. Lower intensities were obtained by attenuating the incident light with neutral density filters.

In a more realistic approximation, hereafter referred to as an "advanced model," the exponential decrease of the laser light intensity inside the semiconductor is accounted for by integrating the PL intensity arising from different depths, as it was explained in Ref. 20. Let us consider a semiconductor layer with thickness L. For generality, we assume that near the surface there is a depletion region with a thickness x_0 in which light is absorbed, but PL is not produced because of the strong electric field.[20] The incident light intensity P_0 decreases inside the semiconductor as $\exp(-\alpha x)$, where x is the distance from the surface. At an

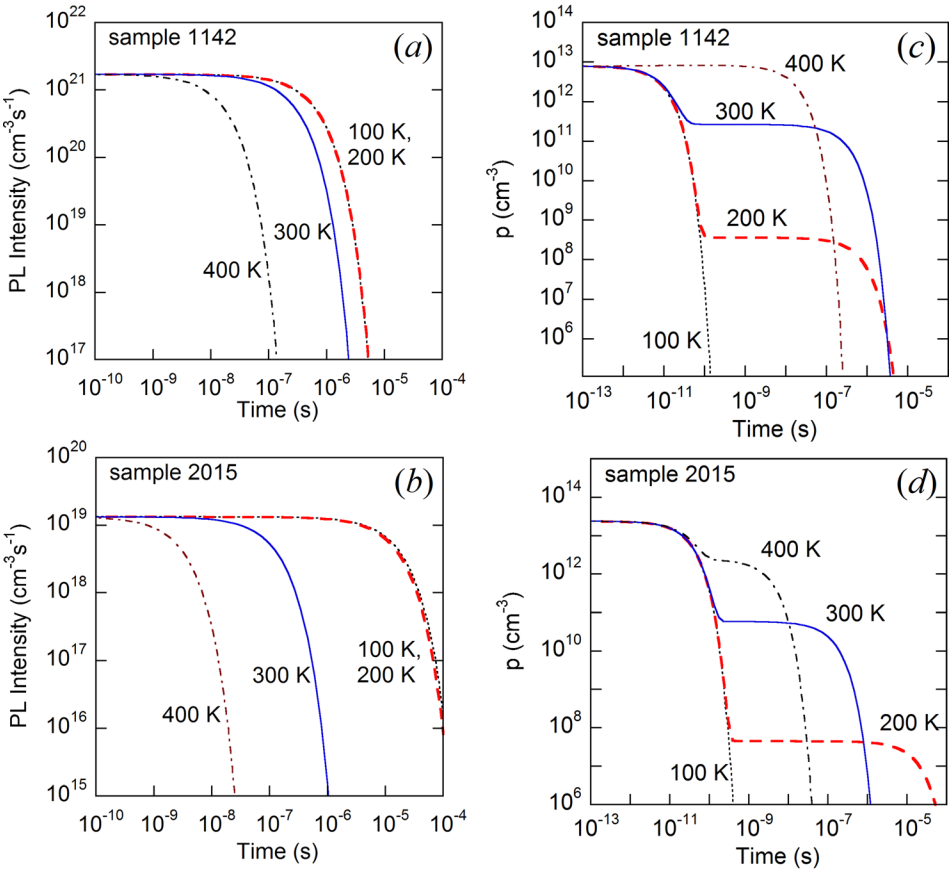

FIG. 13. Calculated decays of PL intensity (for the BL band) and the concentration of free holes by using Eqs. (32) and (33), respectively, with parameters given in Table II. (a) and (b) are the $I_1^{PL}(t)$ dependencies for samples 1142 and 2015, respectively. (c) and (d) are the $p(t)$ dependencies for samples 1142 and 2015, respectively. $C_{p1} = 7 \times 10^{-7}$ cm^3/s, $N_v = 3.2 \times 10^{15} T^{3/2}$ cm^{-3}, $g = 2$, and $G = 10^{24}$ cm^{-3}s^{-1}.

arbitrary distance x, $G(x) = \alpha P_0 \exp(-\alpha x)$. Then, the total intensity of the PL band related to the defect with $i = 1$, which is emitted in all directions from the unit area and from the depth x_0 to L, is

$$I_1^* = \int_{x_0}^{L} \alpha P_0 e^{-\alpha x} \eta_1(x) dx. \tag{36}$$

From Eqs. (21) and (36),

$$I_1^* = \frac{\alpha \eta_{10} P_0}{\tau_{10}} \int_{x_0}^{L} \frac{e^{-\alpha x}}{\lambda} \left\{ 1 - \left(1 - \frac{\lambda \tau_{20}}{2} \right) \exp[-\lambda (t_L - \tau_{20})] \right\} dx, \tag{37}$$

where

$$\lambda = \frac{1}{\tau_{10}} + Q_1 + \frac{\alpha \eta_{10} P_0}{N_1} e^{-\alpha x}. \tag{38}$$

Note that PL intensity given with Eqs. (21) and (32) [or (35)] is expressed as the number of photons emitted from a cubic centimeter, while the PL intensity given with Eq. (37) is expressed as the number of photons emitted from a unit area of a semiconductor layer. When the results calculated in the simple and advanced models are compared, G must be converted into P_0 and $I_1^{PL}(G)$ into $I_1^*(P_0)$ by taking into account that in the simple model $G = \alpha P_0$ and $I^{PL}(G) = \alpha I^*(P_0)$.

Figure 14 shows the dependencies of the peak PL intensity (immediately after a laser pulse) on the excitation intensity for three samples. The experimental dependencies are plotted in relative units. For example, the peak PL intensity was two orders of magnitude higher for sample 1142 than for sample 2015 at very low excitation intensities. In the fits,

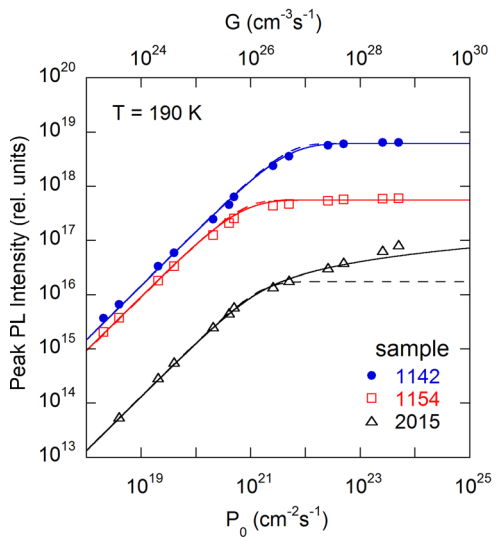

FIG. 14. The dependencies of PL intensity after a laser pulse on excitation intensity. Solid lines are calculated using Eq. (37) (advanced model) with parameters given in Table II. Dashed lines are calculated using Eq. (21) (simple model) with $N_1 = 3.4 \times 10^{17}$, 2×10^{16}, and 3×10^{16} cm^{-3} for samples 1142, 1154, and 2015, respectively. $C_{p1} = 7 \times 10^{-7}$ cm^3/s for all the cases.

obtained by using Eq. (37) and shown with solid curves, we assumed that $x_0 = 0$, because the band bending under illumination at 190 K is significantly reduced, and the depletion region (especially in the degenerate samples) can be ignored. The only fitting parameter was N_1. Other parameters (given in Table II) were obtained from independent experiments. In particular, τ_{10} was directly found from PL decay in time-resolved PL measurements, C_{p1}, E_1, and η_{10} were estimated from analysis of steady-state PL,[7] and Q_1 and τ_{20} were calculated with Eqs. (5) and (8), respectively. The analysis of the calculated dependencies shows that the effect of temperature on the PL intensity after a laser pulse is negligible, i.e., the term $1/Q_1$ in Eqs. (15) and (38) can be ignored. For example, the largest calculated reduction of the PL intensity at highest temperatures used in our experiments was about 5% for samples 1142 and 2015.

At low excitation intensity, the peak PL intensity increases linearly with P_0. At high excitation intensity, a complete saturation is observed for the samples with small thicknesses of the GaN layer co-doped with Si and Zn (1142 and 1154). For the thick GaN layer (2015), slow increase of PL intensity is observed at high excitation intensities, because the region where acceptors become saturated with holes gradually moves deeper and deeper into the thick layer with increasing excitation intensity, in agreement with Eq. (37). For this sample, the dependence calculated with Eq. (21) using the simple model (see dashed line in Fig. 14) disagrees with the experiment, while for the 200 nm-thick layers (samples 1042 and 1154), the fits with the simple model and the advanced model are almost indistinguishable. It is interesting to note that for all of the samples, the value of N_1 is overestimated by a factor of 2–2.5 when it is calculated using the simple model in comparison with the values obtained by using the advanced model.

A very good agreement between theory and experiment demonstrates that time-resolved PL can be used to find the concentrations of acceptors participating in PL in *n*-type semiconductors. Previously, we determined N_1 from steady-state PL only.[7,20] Analysis of the peak PL intensity as a function of the laser intensity in time-resolved PL experiment provides an independent estimate of N_1. The concentrations of the Zn_{Ga} acceptors in the studied GaN samples obtained from the time-resolved PL are given in Table II and compared with data obtained from steady-state PL. We conclude that the accuracy of the PL methods in determining the concentrations of defects is roughly plus-minus half an order of magnitude. The main sources of error are an inaccurate determination of the incident laser intensity in both types of experiments, the assumption that the laser pulse has constant intensity during 1 ns, and an inaccurate estimate of the PL IQE. While the errors due to the first two reasons can be significantly reduced by careful calibration of the experimental setups, possible errors in the IQE require a careful analysis.[21] We would like to note that the accuracy in the determination of the absolute IQE of PL increases significantly for samples with a very high IQE, where the error may be a few percent.[7,21] Such samples can be used as standards for rough estimates of IQE from the external efficiency of PL in different samples measured in identical conditions.

Time-resolved PL can also be used as a contactless method to determine the concentration of free carriers. In Table I, we compare the concentrations of free electrons in *n*-type GaN found from Hall-effect measurements and from time-resolved PL data. In the latter case, n is calculated from Eq. (3) by using the experimentally found τ_{10} and previously determined coefficients C_{n1}. In particular, for the BL band $C_{n1} = (1.5 \pm 0.2) \times 10^{-13}$ cm^3/s, as was found from a set of thin, degenerate GaN layers co-doped with Si and Zn.[7] In some GaN layers grown on sapphire substrates, the concentration of free electrons calculated from room-temperature Hall-effect measurements contains a significant error (up to an order of magnitude), because of a degenerate interfacial region which shunts the conductivity of the main GaN layer.[22] In this case, temperature-dependent Hall-effect measurements with the application of the two-layer model can be used to find the correct value of n.[23] Then, the time-resolved PL method is advantageous and provides a reliable value for the concentration of free carriers in the top 200 nm of the GaN layer.

B. Temperature dependence of PL lifetime and PL intensity

Equation (26) explains the temperature dependence of the PL lifetime (Figs. 6, 8, and 9). At $T < T_0$, the PL signal decays exponentially after a laser pulse, and the PL lifetime τ_1 slowly increasing temperature due to a slow increase of the electron concentration in the conduction band [see Eq. (3) for τ_{10}]. The thermal quenching of PL and an exponential decrease in the measured PL lifetime begin at $T \approx T_0$. In the region of the PL quenching ($T > T_0$), both I_1^{PL} (in steady-state PL measurements) and τ_1 (in time-resolved PL measurements) decrease exponentially with increasing temperature, and the activation energy of this decrease in the Arrhenius plot is close to E_1.

Remarkably, the temperature dependencies of the defect-related PL lifetime and the PL IQE are nearly identical. The latter is described with the following expression:[7,8]

$$\eta_1(T) = \frac{\eta_{10}}{1 + (1 - \eta_{10})\tau_{10}Q_1}, \tag{39}$$

compare this expression with Eq. (26) for $\tau_1(T)$. In experiment, the temperature dependencies of τ_1 and η_1 almost coincide (Figs. 8 and 9), in agreement with Eqs. (26) and (39). The critical temperature T_0 can be defined for both cases as[7]

$$T_0 = \frac{E_1/k}{\ln[(1 - \eta_{10})\tau_{10}Q_1]}. \tag{40}$$

This temperature depends on the absolute IQE of PL and on the PL lifetime for a particular sample, but is independent of the excitation intensity.

A closer inspection shows that the $\eta_1(T)$ and $\tau_1(T)$ dependencies differ by a factor K

$$K = \frac{\eta_1}{\tau_1} = \frac{\eta_{10}}{\tau_{10}}, \tag{41}$$

which has a weak temperature dependence due to the temperature dependence of n in Eq. (3). The weak temperature dependence of τ_{10} can explain the small difference in T_0 when the latter is experimentally determined from the temperature dependencies of either PL intensity or PL lifetime. Figure 15 shows the experimental data for sample 1611. The data are fit with Eqs. (26) and (39), for which a slow exponential rise of the concentration of free electrons with temperature is accounted. The weak dependence of τ_{10} on temperature due to the varying concentration of free electrons has no significant effect on the exponential slope, but explains the small shift of T_0 to lower temperatures for the PL lifetime dependence.

An important conclusion is that the comparison of the temperature dependencies of τ_1 and η_1 can provide information about the possible temperature dependence of the capture coefficients. For example, an independence of η_1 on temperature for $T < T_0$ (where $\eta_1 \approx \eta_{10}$) indicates that C_{p1} is constant or its temperature dependence is negligible [see Eq. (7)]. It can be argued that η_{10} will remain constant if C_{p1} and $\sum_{i=1}^{k} C_{pi}$ have the same temperature dependence. However, such a coincidence is unlikely, especially when the independence of η_{10} on temperature is observed for samples with very different absolute values of η_{10}, for samples grown by different methods and in different doping conditions. On the other hand, the independence of τ_1 on temperature for $T < T_0$ (where $\tau_1 \approx \tau_{10}$) in degenerate samples or a weak dependence on temperature in nondegenerate samples (if it is consistent with the temperature dependence of the free-electron concentration) points to the fact that C_{n1} is constant or its temperature dependence is negligible [see Eq. (3)].

An interesting prediction following from Eq. (33) is that at $T > T_0$, the concentration of free holes decreases after a laser pulse much slower than at $T < T_0$. For example, at room temperature, significant concentration of free holes

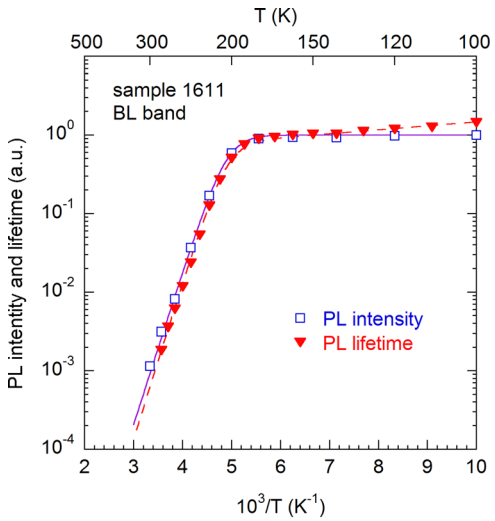

FIG. 15. Temperature dependence of PL intensity and PL lifetime for the BL band in undoped GaN (sample 1611) normalized at 170 K. The solid line is calculated using Eq. (39) with the following parameters: $\eta_{10} = 0.07$, $\tau_{10} = 130$ μs, $E_1 = 348$ meV, and $C_{p1} = 7 \times 10^{-7}$ cm^3/s. The dashed line is calculated with Eq. (26) and the same parameters, with τ_{10} rising as $\exp(-E_D/kT)$, where $E_D = 10$ meV.

should persist up to almost 1 μs after the excitation pulse [Figs. 13(c) and 13(d)]. This effect has the following explanation. During a short excitation pulse, the generated free holes are quickly captured by different defects, in accordance with the absolute IQE of each recombination channel. For example, in sample 1142, about 10^{-11} s after the pulse, 94% of free holes are captured by the Zn_{Ga} acceptors, and the remaining 6% of holes form excitons or are captured by other defects (radiative and nonradiative). However, at room temperature, the holes are efficiently emitted to the valence band from the Zn_{Ga} acceptors during the time period of almost 10^{-6} s [Fig. 13(c)]. These thermally emitted holes keep the concentration of free holes at a sufficiently high level.

C. Temperature dependence of PL lifetime in other models

In early works on PL from defects in semiconductors, the thermal quenching of PL was commonly explained by the Seitz-Mott mechanism.[24,25] According to this mechanism, the PL quenching is caused by a gradual replacement of radiative transitions with non-radiative ones, which involve the same defect (one-center model). The PL decay in this model is expected to be exponential, i.e.,[26,27]

$$I^{PL}(t) = I^{PL}(0)\exp[-(A+R)t]. \tag{42}$$

Here, A is the temperature-independent probability of radiative recombination and R is the probability of the nonradiative recombination, which has a strong temperature dependence. Specifically, $R(T) = R(0)\exp(-E_A/kT)$, where E_A is the energy of the intersecting point in the adiabatic potentials of the excited and ground state of the defect. Although Eq. (42) appears to be similar to Eq. (35), it ignores the competition between different recombination channels and cannot explain the different temperature dependencies of PL lifetime for samples with different IQE of PL.

In fact, for a majority of defects in III-V and II-VI semiconductors, the thermal quenching of defect-related PL occurs via the Schön-Klasens mechanism,[28,29] which involves the thermal emission of charge carriers to the nearest band and the redistribution of these carriers between all other recombination channels.[30] Note that, as in an early work[31] and also in the following papers,[32,33] the Klasens' model was poorly justified, because it involved a nonradiative acceptor (a trap) with a level close to the conduction band and a radiative donor with a level closer to the valence band. This assumption led to the so-called bimolecular law of electron-hole recombination, so that even at high temperatures, the PL decay was expected to occur with a power law[31]

$$I^{PL}(t) \propto (1+at)^{-2}. \tag{43}$$

A very similar law was predicted within the Seitz-Mott mechanism when traps were included into the model.[24,34–36] In the model discussed in Sec. IV, the shallow donor can be regarded as a trap. However, at temperatures above 100 K, the equilibrium (dark) concentration of free electrons in n-type GaN becomes high enough so that the role of the

shallow donor in time-resolved PL becomes insignificant, and the PL decay becomes exponential.

VI. SUMMARY

We have demonstrated that the defect-related PL intensity and PL lifetime have nearly identical temperature dependencies in *n*-type GaN. The differences in these dependencies can be explained by the temperature dependence of the concentration of free electrons, or, otherwise, should be attributed to the temperature dependencies of the carrier-capture coefficients. The PL lifetime decreases above a characteristic temperature, which depends on the internal quantum efficiency of the defect-related PL and the carrier-capture coefficients for the defect. The characteristic PL lifetimes and the lifetime of holes in the valence band can be predicted using a phenomenological model. The same model explains well the dependence of PL intensity on excitation intensity in time-resolved PL experiments. Analysis of this dependence allows us to find the concentrations of defects that participate in PL.

ACKNOWLEDGMENTS

The author is grateful to H. Morkoç (VCU), A. Usikov (TDI, currently at Nitride Crystals Inc.), and A. Bakin (TUBS) for the samples used in this study.

[1]D. G. Thomas, J. J. Hopfield, and W. M. Augustyniak, Phys. Rev. **140**, A202 (1965).
[2]M. A. Reshchikov and H. Morkoç, J. Appl. Phys. **97**, 061301 (2005).
[3]R. Y. Korotkov, M. A. Reshchikov, and B. W. Wessels, Physica B **273–274**, 80 (1999).
[4]R. Y. Korotkov, M. A. Reshchikov, and B. W. Wessels, Physica B **325**, 1 (2003).
[5]M. A. Reshchikov, M. Zafar Iqbal, H. Morkoç, S. S. Park, and K. Y. Lee, Appl. Phys. Lett. **83**, 266 (2003).
[6]M. A. Reshchikov, H. Morkoç, S. S. Park, and K. Y. Lee, Physica B **340–342**, 448–451 (2003).
[7]M. A. Reshchikov, M. A. Foussekis, J. D. McNamara, A. Behrends, A. Bakin, and A. Waag, J. Appl. Phys. **111**, 073106 (2012).
[8]M. A. Reshchikov, A. Kvasov, T. McMullen, M. F. Bishop, A. Usikov, V. Soukhoveev, and V. A. Dmitriev, Phys. Rev. B **84**, 075212 (2011).
[9]Y.-H. Kwon, S. K. Shee, G. H. Gainer, G. H. Park, S. J. Hwang, and J. J. Song, Appl. Phys. Lett. **76**, 840 (2000).
[10]B. Gil, A. Morel, T. Taliercio, P. Lefebvre, C. T. Foxon, I. Harrison, A. J. Winser, and S. V. Novikov, Appl. Phys. Lett. **79**, 69 (2001).
[11]K. D. Glinchuk, K. Lukat, and V. E. Rodionov, Fiz. Tekh. Poluprovodn. **15**, 1337 (1981) [Sov. Phys. Semicond. **15**, 772 (1981)].
[12]G. Davies, T. Gregorkiewicz, M. Zafar Iqbal, M. Kleverman, E. C. Lightowlers, N. Q. Winh, and M. Zhu, Phys. Rev. B **67**, 235111 (2003).
[13]T. Sauncy, C. P. Palsule, M. Holtz, S. Gangopadhyay, and S. Massie, Phys. Rev. B **53**, 1900 (1996).
[14]J. I. Pankove, J. E. Berkeyheiser, and E. A. Miller, J. Appl. Phys. **45**, 1280 (1974).
[15]B. Monemar, H. P. Gislason, and O. Lagerstedt, J. Appl. Phys. **51**, 640 (1980).
[16]W. Shockley and J. W. T. Read, Phys. Rev. **87**, 835 (1952).
[17]V. N. Abakumov, V. I. Perel, and I. N. Yassievich, *Nonradiative Recombinations in Semiconductors* (Elsevier, Amsterdam, 1991).
[18]A. Dmitriev and A. Oruzheinikov, J. Appl. Phys. **86**, 3241 (1999).
[19]J. F. Muth, J. H. Lee, I. K. Shmagin, R. M. Kolbas, H. C. Casey, B. P. Keller, U. K. Mishra, and S. P. DenBaars, Appl. Phys. Lett. **71**, 2572 (1997).
[20]M. A. Reshchikov, Appl. Phys. Lett. **88**, 202104 (2006).
[21]M. A. Reshchikov, "Internal quantum efficiency of photoluminescence in wide-bandgap semiconductors," in *Photoluminescence: Applications, Types and Efficacy*, edited by M. A. Case and B. C. Stout (Nova Science Publishers, Inc., New York, 2012), pp. 1–65.
[22]J. D. McNamara, M. Foussekis, H. Liu, H. Morkoç, M. A. Reshchikov, and A. A. Baski, Proc. SPIE **8262**, 826213 (2012).
[23]D. C. Look and R. J. Molnar, Appl. Phys. Lett. **70**, 3377 (1997).
[24]F. Seitz, Trans. Faraday Soc. **35**, 74 (1939); F. Seitz, *Modern Theory of Solids* (McGraw-Hill, New York, 1940).
[25]R. W. Gurney and N. F. Mott, Trans. Faraday Soc. **35**, 69 (1939); N. F. Mott and R. W. Gurney, *Electronic Processes in Ionic Crystals* (Oxford University Press, London, 1948).
[26]F. A. Kröger, W. Hoogenstraaten, M. Bottema, and T. P. J. Botden, Physica **14**, 81 (1948).
[27]S. Shionoya, "Photoluminescence," in *Luminescence of Solids*, edited by D. R. Vij (Plenum Press, New York, 1998), pp. 95–133.
[28]M. Schön, Z. Phys. **119**, 463 (1942).
[29]H. A. Klasens, Nature **158**, 306 (1946).
[30]M. A. Reshchikov, J. Appl. Phys. **115**, 012010 (2014).
[31]H. A. Klasens and M. E. Wise, Nature **158**, 483 (1946).
[32]W. Hoogenstraaten and H. A. Klasens, J. Electrochem. Soc. **100**, 366 (1953).
[33]H. A. Klasens, J. Phys. Chem. Solids **9**, 185 (1959).
[34]F. Seitz, J. Phys. Chem. Solids **6**, 150 (1938).
[35]F. E. Williams and H. Eyring, J. Chem. Phys. **15**, 289 (1947).
[36]D. Curie, *Luminescence in Crystals* (Methuen, London, 1963), pp. 147–159.